Kinetic Study of Olefin Polymerization with a Supported Metallocene Catalyst. III. Ethylene Homopolymerization in Slurry

S. CHAKRAVARTI, W. HARMON RAY

Department of Chemical Engineering, University of Wisconsin–Madison, Madison, Wisconsin 53706

Received 31 August 2000; accepted 5 October 2000

ABSTRACT: A kinetic study of ethylene homopolymerization is conducted with a supported unbridged metallocene catalyst in a slurry reactor. The effects of operational parameters such as the reaction temperature and pressure on kinetics are investigated. The kinetic parameters which have been determined for this particular catalyst from previous gas phase studies are used in a slurry reactor model to predict the polymerization behavior under various reaction conditions. The experimental data compare favorably with the predictions from this model. © 2001 John Wiley & Sons, Inc. J Appl Polym Sci 81: 2901–2917, 2001

Key words: ethylene homopolymerization; metallocene catalyst; kinetic study

INTRODUCTION

Slurry reactors, rather than gas-phase reactors, are used on a wider scale in industrial laboratories for catalytic olefin polymerization studies. But gas-phase reactors are increasingly being used for the commercial production of polyolefins due to their significant process advantages. Discrepancies can arise when comparing results for the same catalyst run in a gas-phase reactor and in a slurry reactor. The following study was motivated by a need to demonstrate how to unify slurry and gas-phase kinetics.

This is the third part in the series of articles on the kinetics of supported metallocenes. In Part I,[1] a kinetic study on ethylene homopolymerization and ethylene–propylene copolymerization in a laboratory-scale gas-phase reactor was conducted using an unbridged zirconocene on a silica support. The temperature and comonomer effects were investigated and perturbation techniques were implemented to estimate important kinetic parameters. Using POLYRED™, models were proposed and the predictions compared well with the experimental data under various reaction conditions. Hence, a kinetic model adequate for continuous reactor design and scale-up was achieved. In Part II,[2] ethylene-1-hexene copolymerization in the gas phase was investigated with the same catalyst used in Part I. Using a similar experimental methodology as in Part I, a comparison of the kinetic behavior and parameters of the two ethylene–comonomer systems was possible. Some of the significant results that were obtained include (i) the reaction-rate order of ethylene in the presence of the comonomer (irrespective of its type) was found to be close to 1, while it was found to be closer to 2 in the absence of the comonomer and (ii) ethylene displayed higher activity in the presence of propylene as compared to 1-hexene for this particular catalyst. In Part III, we now compare the behavior of this catalyst in different reactor systems. The kinetics of ethylene homopolymerization is studied in a slurry reactor. The

Correspondence to: W. H. Ray.

Journal of Applied Polymer Science, Vol. 81, 2901–2917 (2001)

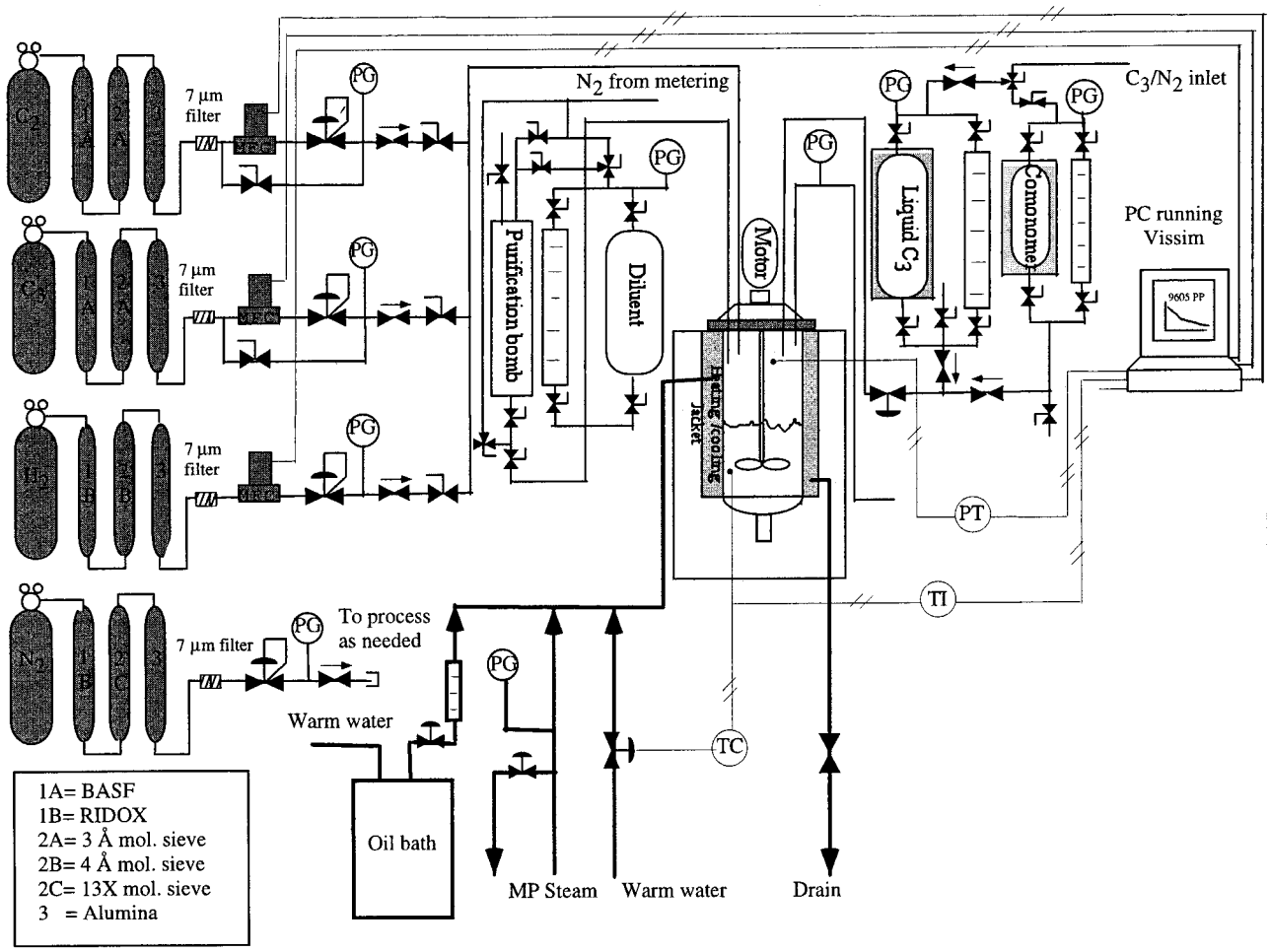

Figure 1 Slurry reactor system.

kinetic parameters obtained from the gas-phase reactor in Part I are used in a slurry reactor model to predict the behavior under various reaction conditions. The model predictions are then compared to the experimental data obtained in the slurry reactor.

The stirred-bed reactor (SBR) system built at the UWPREL[3] is designed to study the gas-phase kinetics of ethylene–comonomer systems such as ethylene/propylene (E–P) and ethylene/1-hexene (E/1-H). This gas-phase reactor was well described in previous investigations with supported metallocenes and traditional Ziegler–Natta catalysts.[4–6]

The slurry reactor was built in 1993[7] and is currently being used to conduct ethylene homopolymerization reactions. The reactor system facilitates diluent-based or liquid pool polymerizations.

EXPERIMENTAL

The slurry reactor system has been used previously to conduct reactions with traditional Ziegler–Natta catalysts.[7] A schematic of the system is shown in Figure 1 and the various ports on the reactor vessel are shown in Figure 2. The reactor vessel is a 4-L Zipperclave reactor manufactured by Autoclave Engineers. The gas-purification system in the slurry setup is very similar to what is present in the gas-phase reactor system. The gaseous monomers, hydrogen and nitrogen, are subject to triple purification to get rid of oxygen, moisture, and other impurities. High-purity heptane (HPLC grade) is used as the diluent in the reactions. The heptane is poured into a purification column containing molecular sieves for no less than 24 h prior to being used in a reaction. Prior to conducting the reaction, the following preparation procedure is instituted:

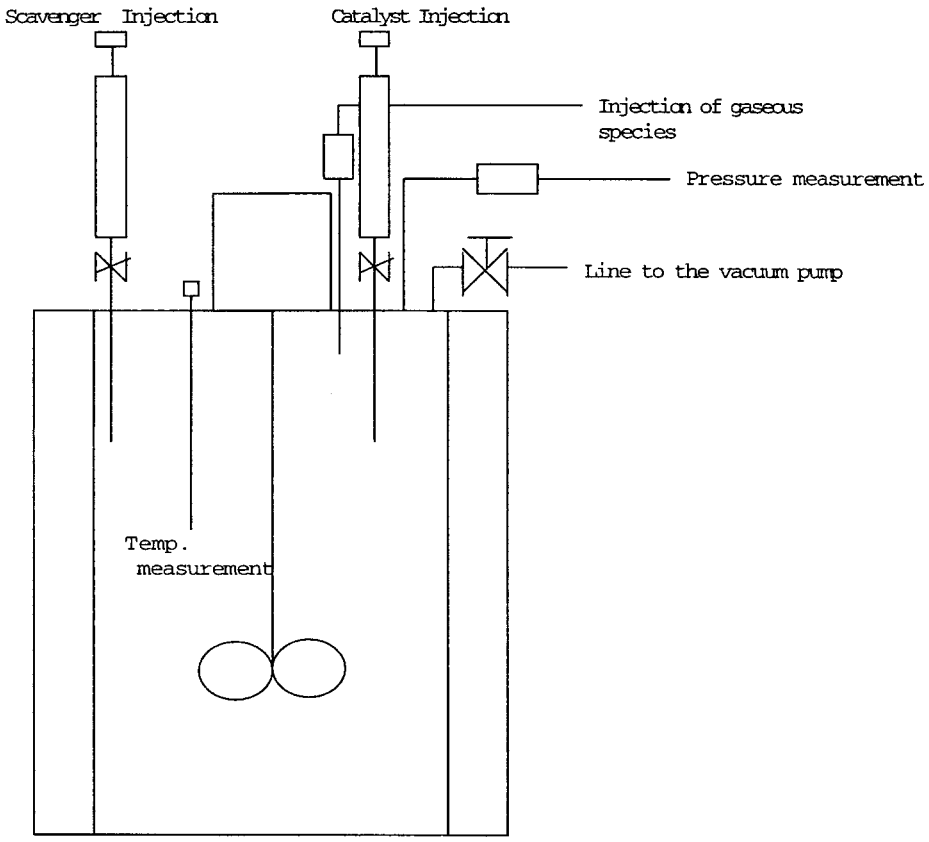

Figure 2 Schematic of the slurry reactor vessel.

- On the day before the reaction, the reactor is evacuated at 90°C for about 2 h, following which the reactor is pressurized with ultra-high-pure (UHP) nitrogen overnight to check for the presence of any leaks in the reactor system.
- On the following day, the reactor is subject to a 1-h heat evacuation at 90°C.
- On completion of the heat-evacuation cycle, heptane is introduced into the reactor and the magnetically driven motor is set to a stirrer speed of about 1200 rpm.
- The temperature is then increased to the desired set-point. The temperature is controlled by passing steam and water through the cooling jacket of the reactor vessel.
- Ethylene is introduced into the system after the temperature has reached the desired set-point. Ethylene flow into the system is not stopped until vapor–liquid equilibrium has been achieved.
- Following that, the scavenger [triethylaluminum (TEA) in a heptane solution] is introduced into the system. The scavenging time is approximately 15 min.
- The catalyst is introduced into the reactor on completion of the scavenging procedure. Ethylene is used to inject both the scavenger and the catalyst. Once the catalyst is introduced, the ethylene flow is started with computer data logging.

The presence of the thermocouple and the pressure transducer facilitate online monitoring of the temperature and pressure during the course of a reaction. During this "no-purge" mode operation, the pressure is maintained by the constant flow of the monomer.

SLURRY KINETICS

The primary objective of the current study was to capture the kinetic behavior in slurry reactors using a model with parameters estimated from gas-phase studies. To observe kinetics under various reaction

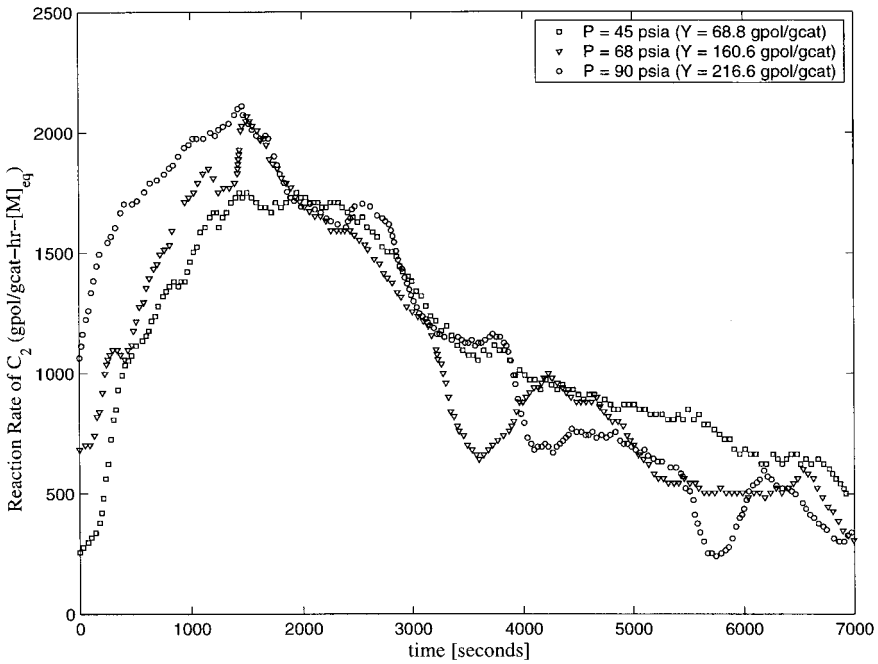

Figure 3 Pressure effects at 70°C.

conditions, the slurry experiments were conducted in the pressure range of 3–6 atm and a temperature range of 60–80°C. Compared to gas-phase kinetics, there are a variety of issues that need to be dealt with when trying to analyze slurry kinetics:

- Gas–liquid mass-transfer limitations: The transfer of ethylene from the gas phase to the liquid phase can prove to be rate-limiting if it is slower than is the reaction rate in the liquid phase. Changes in various operational factors such as pressure, temperature, solids concentrations, and stirrer speeds affect the gas–liquid mass-transfer rate. The gas–liquid mass-transfer coefficient, $k_L a$, provides a measure of the severity of these mass-transfer limitations. Hence, the effects of the aforementioned factors on $k_L a$ are examined.
- Determination of the equilibrium concentration of the monomer in the diluent and the polymer: The Benedict–Webb–Rubin (BWR) equation is used to determine the ethylene concentration in the diluent. Flory[8] equations are used to determine the concentrations of the various species in the polymer phase.
- Presence of diffusion limitations: Floyd et al.[9] studied the importance of mass- and heat-transfer limitations during polymer particle growth using the multigrain model. The presence of diffusion limitations at the macroparticle level early on in the lifetime of the polymer particle in slurry reactions was predicted to be present irrespective of the operating conditions. Hence, the presence of diffusion limitations is considered in the slurry reactor model.

Experimental Observations

A total of 10 experiments were conducted to study (i) the pressure effects at 70 and 80°C and (ii) the temperature effects at pressures of 55 and 90 psia. The experiments to be conducted include

- Pressure effects

  1. 70°C—45, 55, 68, 90 psia
  2. 80°C—45, 55, 68, 90 psia.

- Temperature effects

  1. 55 psia—60, 70, 80°C
  2. 90 psia—60, 70, 80°C.

The reaction-rate data is presented as gpol/gcat^{-1} h^{-1} $[M^{-1}]_{eq}$. The procedure implemented to determine the equilibrium monomer concentration in the polymer, $[M]_{eq}$, will be described in a later section.

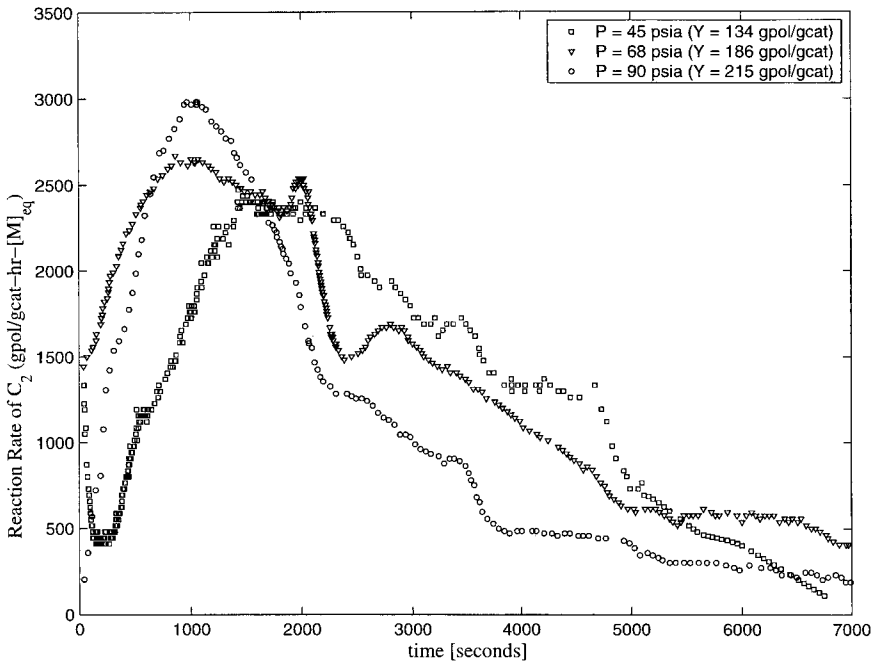

Figure 4 Pressure effects at 80°C.

- Pressure effects: Figures 3 and 4 illustrate the kinetics observed by varying the reactor pressure at 70 and 80°C. The profiles obtained at the different pressures for a given reactor temperature are very similar because the reaction rates were normalized by the equilibrium ethylene concentration in the polymer. Thus, if the observed polymerization reaction rate were first order in ethylene, all curves are expected to be the same. The fact that the normalized yield does increase with the reactor pressure suggests a reaction-rate order greater than 1 for ethylene homopolymerization as was found in our earlier gas-phase studies.[1]
- Temperature effects: The kinetics obtained at the different temperatures for pressures of 55 and 90 psia are shown in Figures 5 and 6. While the peak position fails to change noticeably with an increase in the reaction temperature, the peak value and the decay rate do increase with an increase in the temperature as expected. An overall enhancement in activity is observed with an increase in the temperature. The increase in the decay rate with an increase in the temperature is more pronounced when the reaction pressure is maintained at 90 psia.

Determination of the Gas–Liquid Mass-transfer Coefficient

The importance of gas–liquid mass-transfer effects in slurry and solution polymerizations was emphasized in previous investigations.[10–15] Factors that can influence the rate of the mass transfer of ethylene from the gas phase into heptane include temperature, pressure, solids concentration, and stirrer speeds. Morsi et al.[13] used a statistical approach to investigate the effects of the aforementioned factors on the mass-transfer coefficient of ethylene into *n*-hexane. They found pressure to have a negligible effect on the k_La for ethylene transfer into *n*-hexane. Also, the k_La values increased slightly at small solid concentrations ($\leq$15 mass %) and then sharply decreased when the solids concentration exceeded 30 mass %. An increase in temperature was found to have a slight increase in the value of the mass-transfer coefficient.[13] However, this and other studies[11,15] showed that, of all the factors, the stirrer speed exerted the greatest influence on the gas–liquid mass transfer; k_La increased significantly when the agitator speed was increased. Based on the above conclusions, the consideration of the effects of the different factors on k_La in the present investigation are summarized:

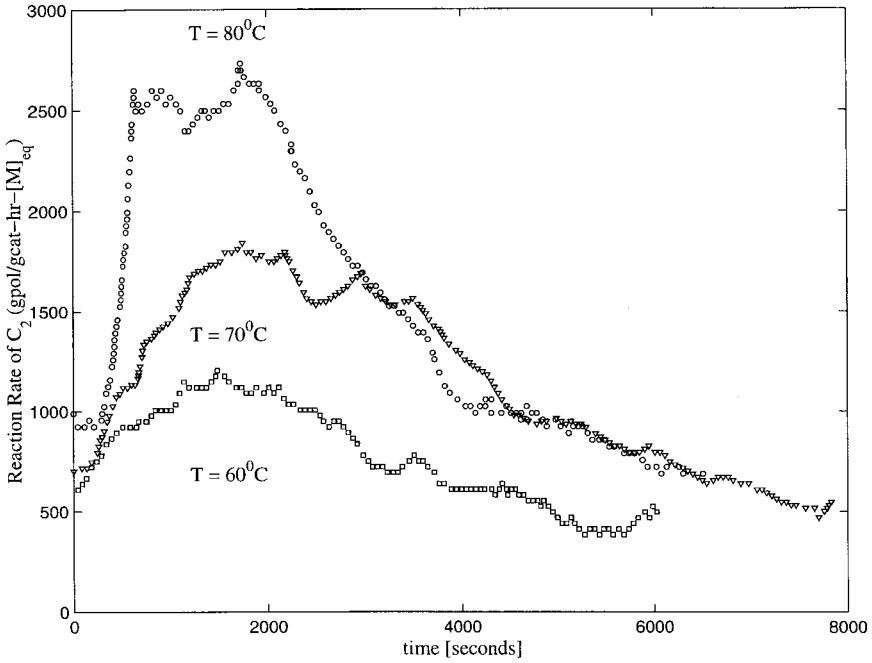

Figure 5 Temperature effects at 55 psia.

- The stirrer speed was maintained at 1200 rpm for all the reactions conducted in this work (the maximum stirrer speed possible without overheating the motor).
- The effect of pressure on mass-transfer effects is assumed to be negligible.
- The solids concentrations in the diluent are not very high for the reactions conducted since 1.5 L of the solvent is used and the catalyst amount is adjusted such that the amount of the polymer collected does not exceed 30–40 g. Hence, the impact of this variable on k_La is assumed to be minimal.
- The effect of temperature on k_La was studied

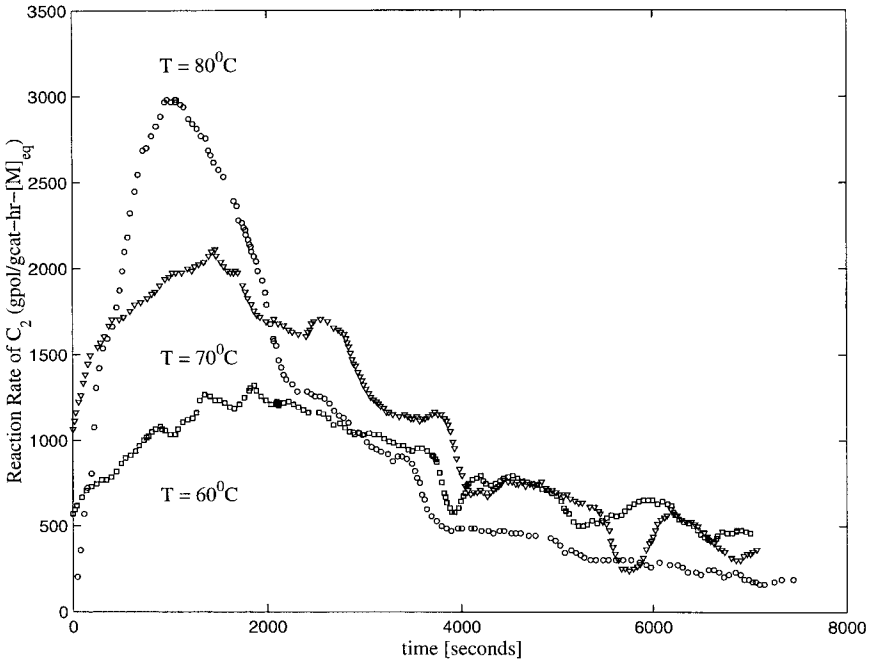

Figure 6 Temperature effects at 90 psia.

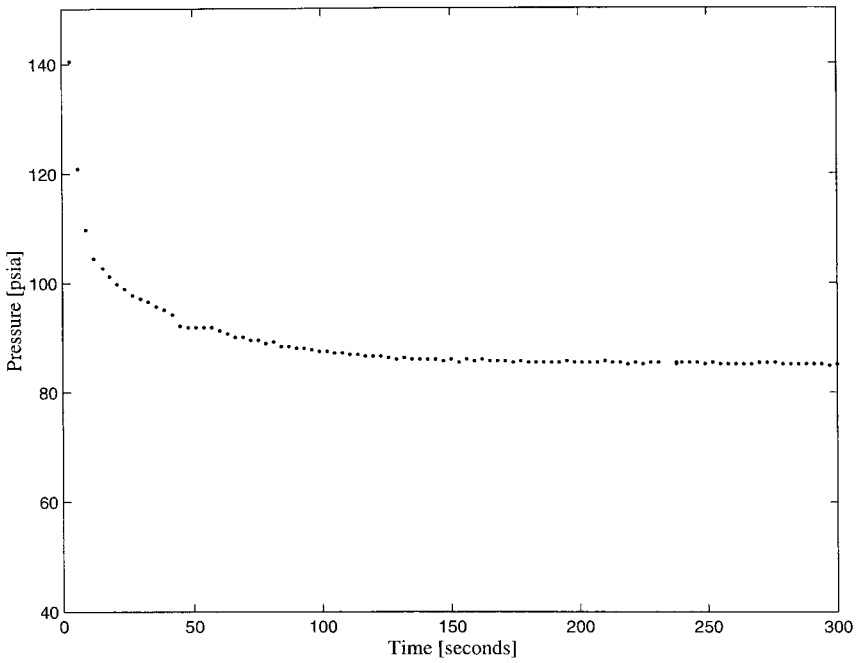

Figure 7 Pressure as a function of time (1200 rpm).

and is discussed in the latter part of this section.

Previous researchers have, with some success, used various empirical correlations involving dimensionless numbers to estimate k_La.[11,14,15] In the current effort, the experimental technique implemented to determine the mass-transfer coefficient is based on the physical absorption technique used by Chang and Morsi.[10] This technique was used by Mallon[15] in our laboratory to study mass-transfer effects in solution ethylene polymerization. To summarize this technique, consider the mass balance for ethylene in the reactor:

$$\frac{dm}{(Mw)dt} = \frac{d(v_g p)}{(RT)dt} = F_{\text{in}} - F_{\text{out}} - k_L a([M_1]_{\text{eql}} - [M_1]_{\text{liq}})V_{\text{liq}} \quad (1)$$

where m is the mass of ethylene; Mw, the molecular weight of ethylene; $[M_1]_{\text{eql}}$, the equilibrium monomer concentration in the liquid; and $[M_1]_{\text{liq}}$, the bulk concentration of ethylene in the liquid.

The following assumptions were made in eq. (1): (i) ideal gas behavior for ethylene and (ii) constant liquid-phase volume. Due to the semibatch operation, outflow does not exist. To observe pure mass-transfer effects, ethylene is fed such that the reactor is pressurized to the desired value and the flow into the reactor is stopped after that. As a result, the mass-balance equation simplifies to

$$\underbrace{\frac{dp}{dt}\left(\frac{v_g}{RTV_{\text{liq}}}\right)}_{y} = \underbrace{-k_La}_{m}\underbrace{([M_1]_{\text{eql}} - [M_1]_{\text{liq}})}_{x} \quad (2)$$

k_La is the slope of the line when "y" is plotted versus "x." For a typical run, the following steps are performed:

- The diluent (heptane) is charged into the reactor.
- The reactor is then pressurized with ethylene and is heated to the desired temperature.
- When the stirrer (set to the desired mixing speed) is turned on, the computer simultaneously starts recording the change in pressure with time.

Figure 7 shows the change in pressure over time as recorded by the computer. The corresponding least-squares plot obtained is shown in Figure 8(a). The equilibrium monomer concentration in heptane at the different pressures is calculated by the BWR vapor–liquid equilibrium equation.[15] The bulk concentration of the

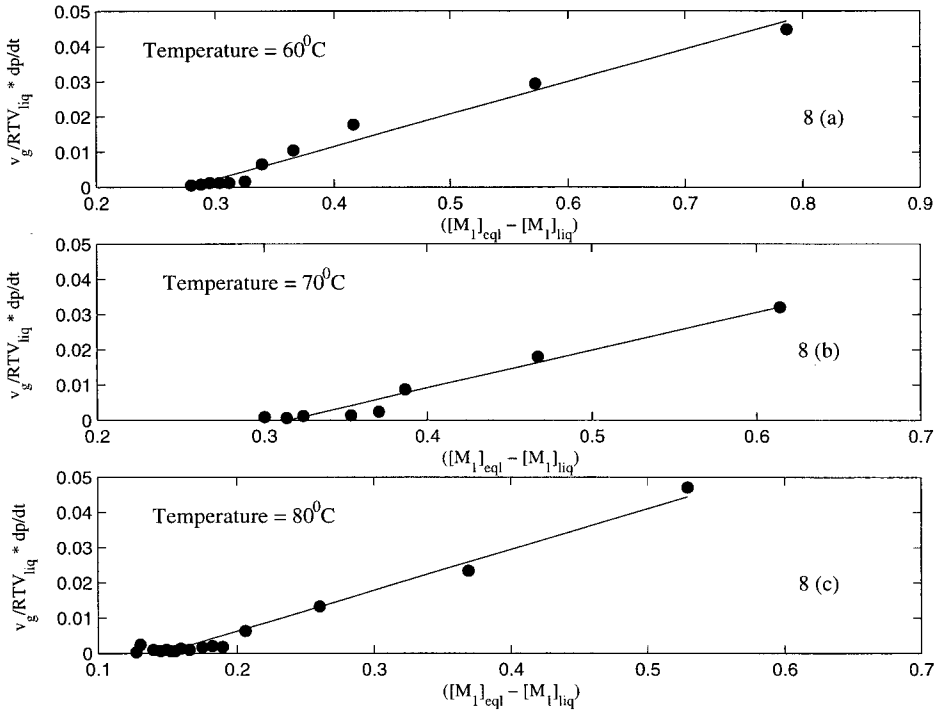

Figure 8 Least-squares fit for $k_L a$ at the different reaction temperatures.

monomer in the liquid may be seen in Figure 9 based on temperature and pressure in the gas phase. The effect of temperature on the gas–liquid mass-transfer coefficient is shown in Table I. The least-squares fits obtained when determining $k_L a$ at the various temperatures are

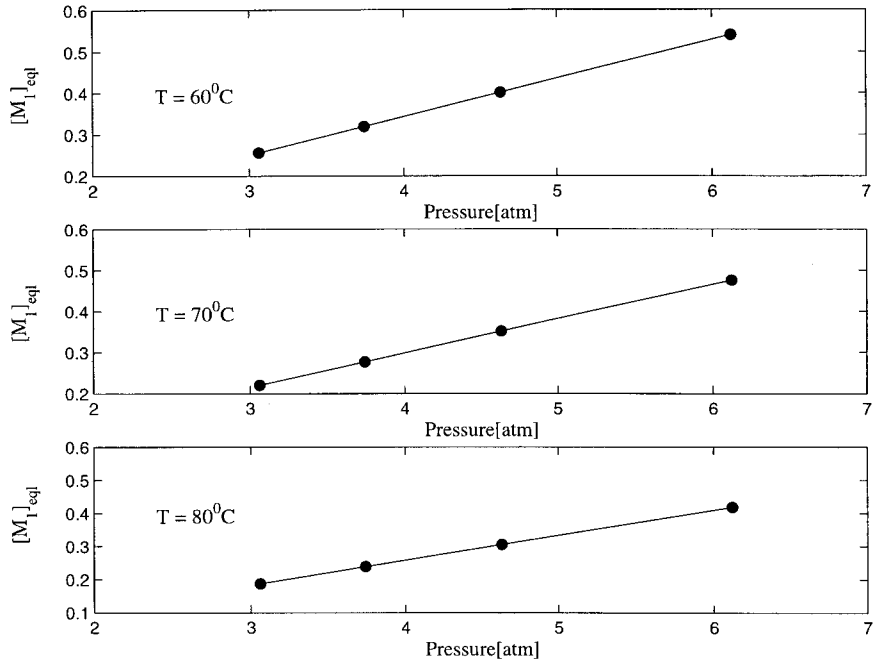

Figure 9 BWR results: Equilibrium ethylene concentration in heptane as a function of partial pressure.

Table I Effect of Temperature on k_La

Temperature (K)	k_La (s^{-1})
333	0.09
343	0.103
353	0.115

shown in Figure 8. The results show that the coefficient increases slightly with an increase in temperature, which is quite consistent with what has been observed previously.[10,13]

Determination of the Equilibrium Monomer Concentration in the Polymer

Various correlations such as Henry's law[13,17] or the BWR equation can be used to ascertain the concentration of ethylene in heptane. Hutchinson[18] successfully used the BWR equation to fit experimental data from the literature for the ethylene–heptane system over a wide range of pressures. Hence, this equation is used in determining the concentration of ethylene in heptane for the various reaction conditions considered. The concentrations for the various species in the polymer phase are determined using the Flory equations[18] for a ternary system consisting of a single polymer component in a binary solvent mixture. To determine the concentrations in the polymer phase, equilibrium between phases needs to be attained. In the current investigation, the three conditions for equilibrium between the two phases are said to be satisfied:

$$\mu_{1p} = \mu_{1s}$$
$$\mu_{2p} = \mu_{2s}$$
$$\mu_{3p} = \mu_{3s} \quad (3)$$

where

- s is the solvent phase
- p is the polymer phase
- 1 is ethylene, 2 is heptane, and 3 is the polymer.

The equations for the derivation of the chemical potentials can be put in the form shown in Eqs. (4)–(6):

Table II Comparison of Partition Coefficients for the Different Reaction Conditions

Pressure (atm)	Temperature (°C)	Partition Coefficient (K_l)
3.06	70	0.225
3.06	80	0.243
3.74	60	0.216
3.74	70	0.222
3.74	80	0.224
4.63	70	0.217
4.63	80	0.225
6.12	60	0.197
6.12	70	0.204
6.12	80	0.211

$$\mu_1 - \mu_1^0 = RT\left[\ln v_1 + (1 - v_1) - v_2\left(\frac{x_1}{x_2}\right) - v_3\left(\frac{x_1}{x_3}\right) + (\chi_{12}v_2 + \chi_{13}v_3)(v_2 + v_3) - \chi_{23}\left(\frac{x_1}{x_2}\right)v_2v_3\right] \quad (4)$$

$$\mu_2 - \mu_2^0 = RT\left[\ln v_2 + (1 - v_2) - v_1\left(\frac{x_2}{x_1}\right) - v_3\left(\frac{x_2}{x_3}\right) + (\chi_{21}v_1 + \chi_{23}v_3)(v_1 + v_3) - \chi_{13}\left(\frac{x_2}{x_1}\right)v_1v_3\right] \quad (5)$$

$$\mu_1 - \mu_1^0 = RT\left[\ln v_3 + (1 - v_3) - v_1\left(\frac{x_3}{x_1}\right) - v_2\left(\frac{x_3}{x_2}\right) + (\chi_{31}v_1 + \chi_{32}v_2)(v_2 + v_1) - \chi_{12}\left(\frac{x_3}{x_1}\right)v_2v_1\right] \quad (6)$$

where

- x_1, x_2, and x_3 represent the number of segments per molecule in the respective species. They can be substituted for by their respective molar volumes.
- χ_{ij} are the interaction parameters between the different species involved. The following relationship is used to determine χ_{ji}:

Table III Elementary 1-Site Reaction-rate Model for Homopolymerization

Name	Reaction
Activation	$C_{\text{pot}} + M \rightarrow C_o^*$
Propagation	$C_n^* + M \rightarrow C_{n+1}^*$
Deactivation	$C_n^* \rightarrow C_d + D_n$

Table IV Kinetic Parameters for Homopolymerization

Parameter	Estimated Value	Units
Preexponential factors		
Site activation, $k_{ao}C_{pot}$	0.74×10^{1}	cc-amor.polym. g^{-1} cat^{-1} s^{-1}
Propagation, $k_{po}C_{pot}$	1.5×10^{10}	cc-amor.polym. g^{-1} cat^{-1} s^{-1}
Deactivation, k_{do}	1.9×10^{7}	s^{-1}
Activation energies		
Site activation, E_a	4.54	kcal/mol
Propagation, E_p	13.87	kcal/mol
Deactivation, E_d	16.90	kcal/mol

$$\chi_{ji} = \chi_{ij}\left(\frac{x_j}{x_i}\right) = \chi_{ij}\left(\frac{V_j}{V_i}\right) \tag{7}$$

where V_j and V_i are the partial molar volumes of the species j and i, respectively.

- v_1, v_2, and v_3 are the volume fractions of species 1, 2, and 3, respectively.

The partial molar volumes are determined by the method of Chueh and Prausnitz[19] which uses a modified Redlich–Kwong equation. Equations (8) and (9) show how χ_{12} (refs. 20–22) and χ_{23} (ref. 18) were determined. χ_{13} was obtained from the *Handbook of Polymer–Liquid Interaction Parameters and Solubility Parameters.*[23] χ_{13} used in the calculations was considered to be constant at 0.3:

$$\chi_{12} = 0.5 - \psi\left(1 - \frac{\theta}{T}\right) \tag{8}$$

$$\chi_{23} = \left(\frac{V_2}{RT}\right)(\delta_2 - \delta_3)^2 + \gamma \tag{9}$$

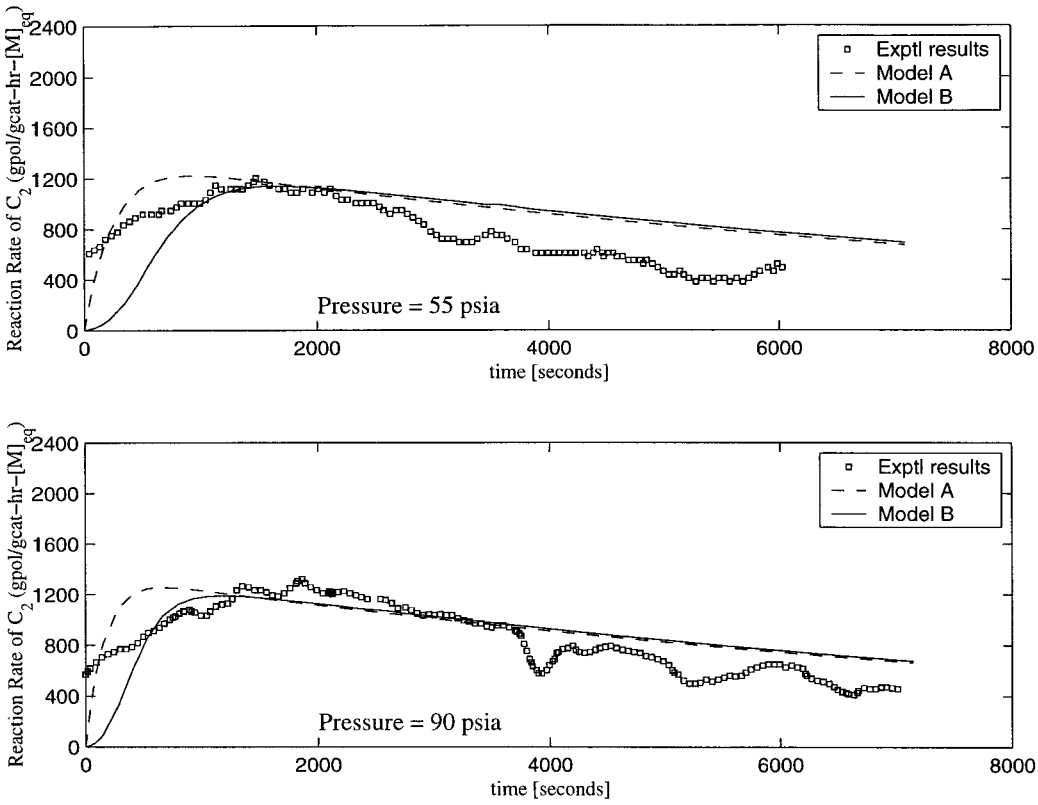

Figure 10 Model predictions versus experimental data at 60°C. Model A: Includes gas–liquid mass-transfer limitations. Model B: Accounts for gas–liquid mass-transfer and diffusion limitations.

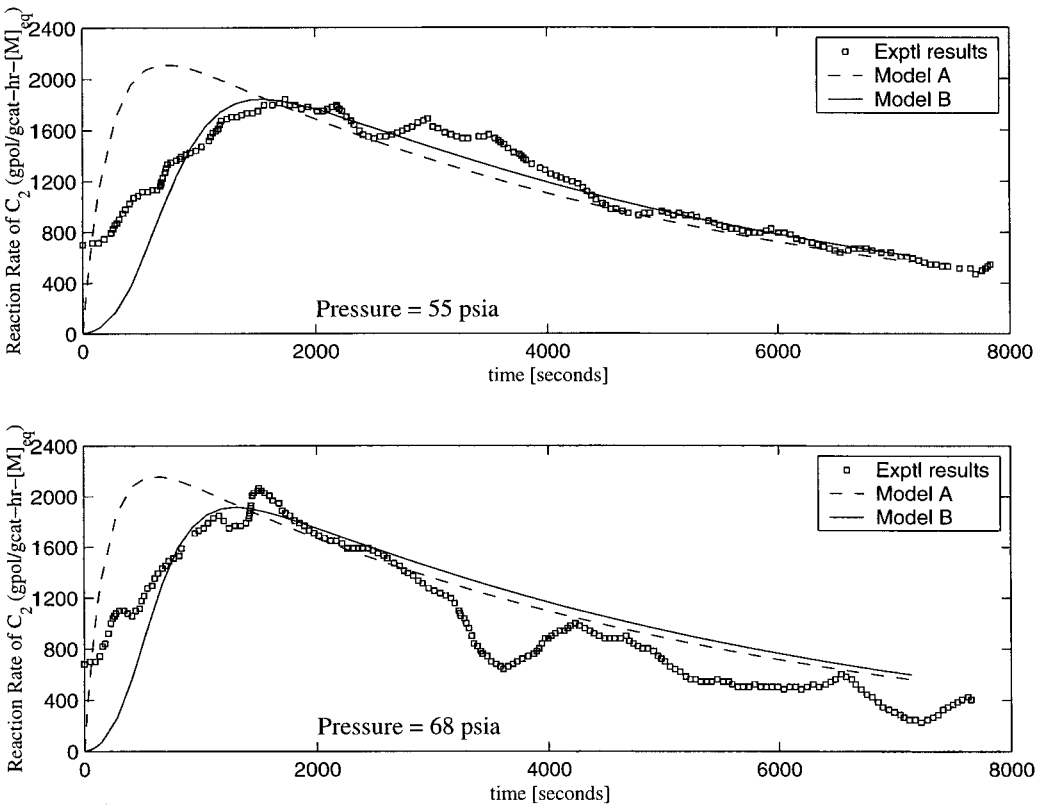

Figure 11 Model predictions versus experimental data at 70°C. Model A: Includes gas–liquid mass-transfer limitations. Model B: Accounts for gas–liquid mass-transfer and diffusion limitations.

where (i) ψ, the entropy parameter,[22] and θ, known as the *theta* (or *Flory*) *temperature,*[22] were obtained from previous studies with the values of −3.58 and 485 K, respectively, and (ii) γ is an entropy correction term considered to be constant near 0.3 when the polymer is one of the components in the pair.[17] For the current problem, it is assumed that the volume fraction of the polymer in the solvent phase is small enough such that it is negligible. With that, the equations used in determining the volume fractions for the various components in the polymer phase are shown in eqs. (10)–(12). Based on the information obtained from the volume fractions, it is possible to determine the monomer concentration in the polymer phase at the different reaction conditions:

$$RT\Bigg[\ln v_1 + (1 - v_1) - v_2\left(\frac{x_1}{x_2}\right) - v_3\left(\frac{x_1}{x_3}\right) + (\chi_{12}v_2 + \chi_{13}v_3)(v_2 + v_3) - \chi_{23}\left(\frac{x_1}{x_2}\right)v_2v_3\Bigg] - \mu_{1s} = 0 \tag{10}$$

$$RT\Bigg[\ln v_2 + (1 - v_2) - v_1\left(\frac{x_2}{x_1}\right) - v_3\left(\frac{x_2}{x_3}\right) + (\chi_{21}v_1 + \chi_{23}v_3)(v_1 + v_3) - \chi_{13}\left(\frac{x_2}{x_1}\right)v_1v_3\Bigg] - \mu_{2s} = 0 \tag{11}$$

$$v_1 + v_2 + v_3 - 1 = 0 \tag{12}$$

Based on the knowledge of its volume fraction in the polymer phase (v_i) and the partial molar volume (V_i), the equilibrium monomer concentration ($[M_i]_{eq}$) of monomer i in the polymer phase can calculated:

$$[M_i]_{eq} = \frac{v_i}{V_i} \tag{13}$$

The equilibrium monomer concentration in the diluent ($[M_i]_{eql}$) is calculated using the BWR equation. The partition coefficient (K_l) for monomer i is therefore defined as

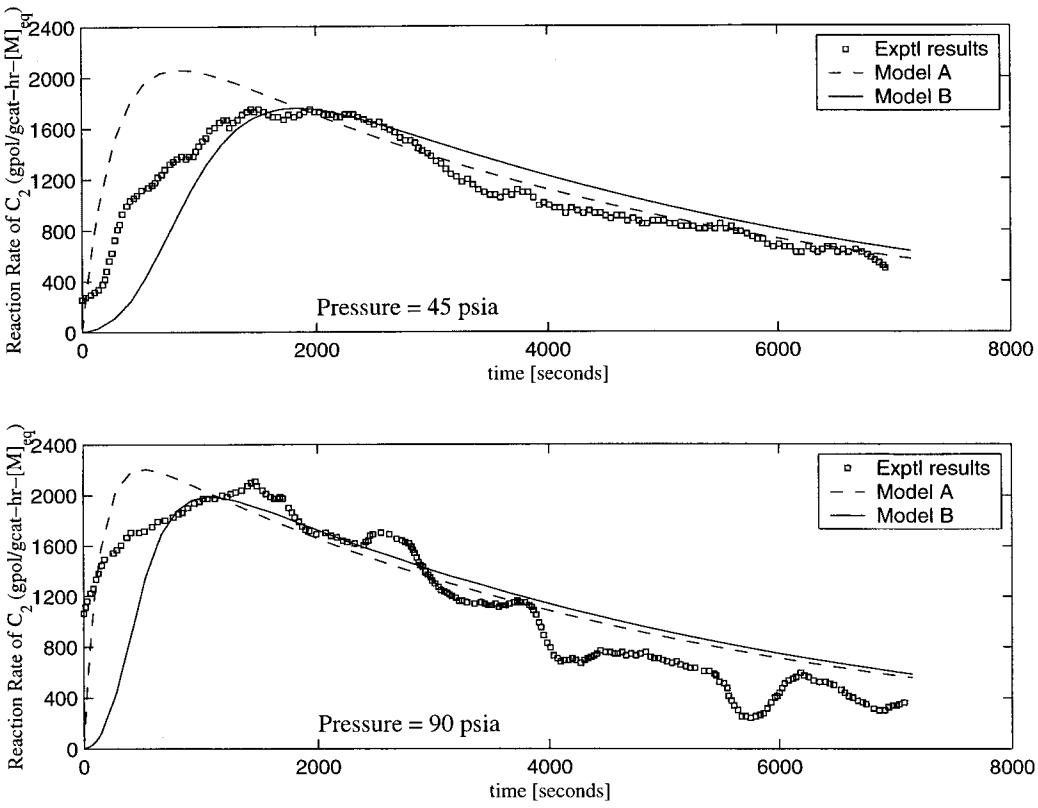

Figure 12 Model predictions versus experimental data at 70°C. Model A: Includes gas–liquid mass-transfer limitations. Model B: Accounts for gas–liquid mass-transfer and diffusion limitations.

$$K_l = \frac{[M_i]_{\text{eq}}}{[M_i]_{\text{eql}}} \tag{14}$$

Table II contains the partition coefficients that have been calculated at the different operating conditions.

Role of Diffusion

Floyd et al.[9] conducted theoretical investigations on the effects of intraparticle heat and mass transfer for a range of catalyst activities in slurry and gas-phase reactors. The multigrain (MGM) model was implemented to investigate the mass- and heat-transfer effects at the macroparticle and microparticle levels. Some of the important conclusions for slurry polymerization are summarized[9]:

- Thermal gradients are negligible at the microparticle level and for most operating conditions at the macroparticle level.
- Concentration gradients
  - Can be significant at the microparticle level for high-activity catalysts and for those yielding large primary crystallites after breakup.
  - Are usually significant at the macroparticle level, especially early in the lifetime of the polymer particle.

Based on the conclusions put forth by Floyd et al.,[9] the following assumptions are made for the present study:

- Negligible heat- and mass-transfer limitations at a microparticle level.
- Negligible intraparticle temperature gradients in the macroparticle under normal operating conditions.

The assumption of negligible intraparticle temperature gradients leads to the following solution for the isothermal reaction-diffusion problem for the macroparticle[9]:

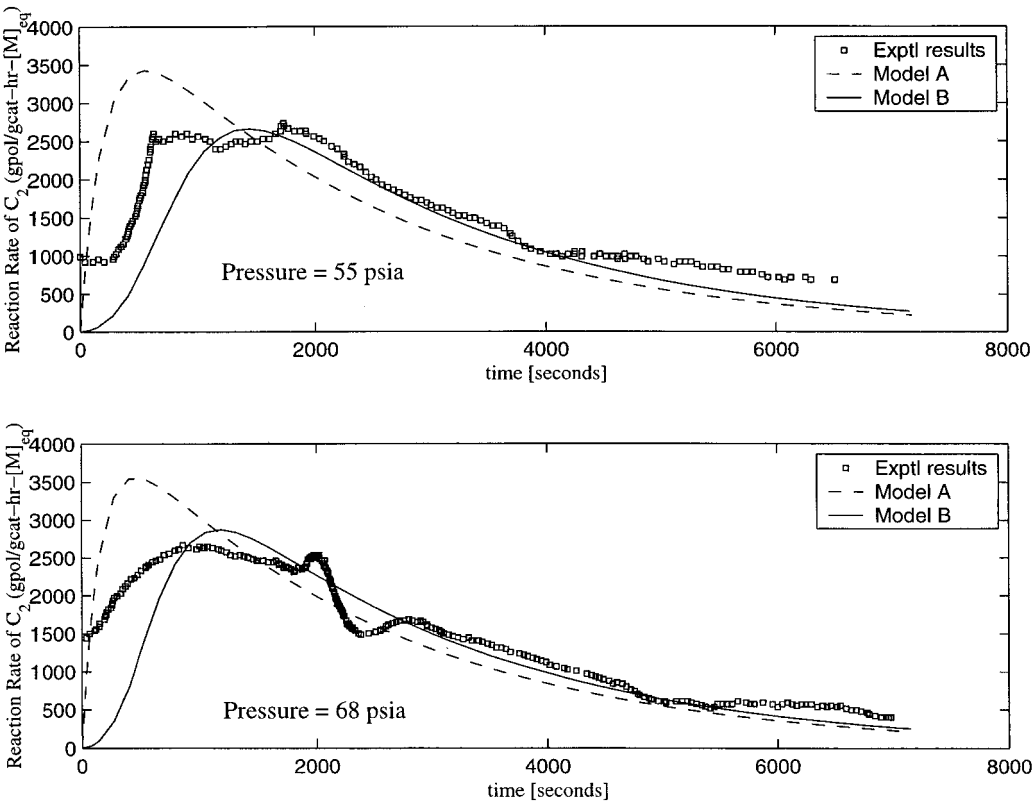

Figure 13 Model predictions versus experimental data at 80°C. Model A: Includes gas–liquid mass-transfer limitations. Model B: Accounts for gas–liquid mass-transfer and diffusion limitations.

$$\eta_l = \frac{3}{\alpha_l}\left[\frac{1}{\tanh(\alpha_l)} - \frac{1}{\alpha_l}\right] \tag{15}$$

where η_l is the macroparticle effectiveness factor. The Thiele modulus, α_l, is determined by the following equation[9]:

$$\alpha_l = \frac{d_{\text{cat}}}{2}\,\phi\sqrt{\frac{k_p C_{\text{act}}}{\phi^3 D_l}} \tag{16}$$

where d_{cat} is the diameter of the catalyst particle; k_p, the kinetic constant for propagation; C_{act}, the concentration of active sites; and D_l, the macroparticle diffusivity. The growth factor, ϕ, is determined by

$$\phi = \sqrt[3]{\frac{\rho_{\text{cat}}}{\rho_{\text{pol}}}\,\text{Yield} + 1} \tag{17}$$

where ρ_{cat} is the density of the catalyst, and ρ_{pol}, the density of the polymer. The observed reaction rate can then be determined from $R_{\text{obs}} = \eta_l R_{\text{kin}}$, where η_l is calculated by eq. (15).

Slurry Kinetic Model

The kinetic mechanism for this catalyst was already presented, but is summarized in Table III. The equations used in the slurry model are outlined below:

$$\rho_{\text{mix}}\frac{dV}{dt} = -V\frac{d\rho_{\text{mix}}}{dt} + k_L a([M_1]_{\text{eql}} - [M_1]_{\text{liq}})MwV_{\text{liq}} \tag{18}$$

$$V\frac{d[M_1]_b}{dt} = Rate\ V + k_L a([M_1]_{\text{eql}} - [M_1]_{\text{liq}})V_{\text{liq}} - [M_1]_b\frac{dV}{dt} \tag{19}$$

$$V\frac{dC_{\text{cat}}}{dt} = -C_{\text{cat}}\frac{dV}{dt} \tag{20}$$

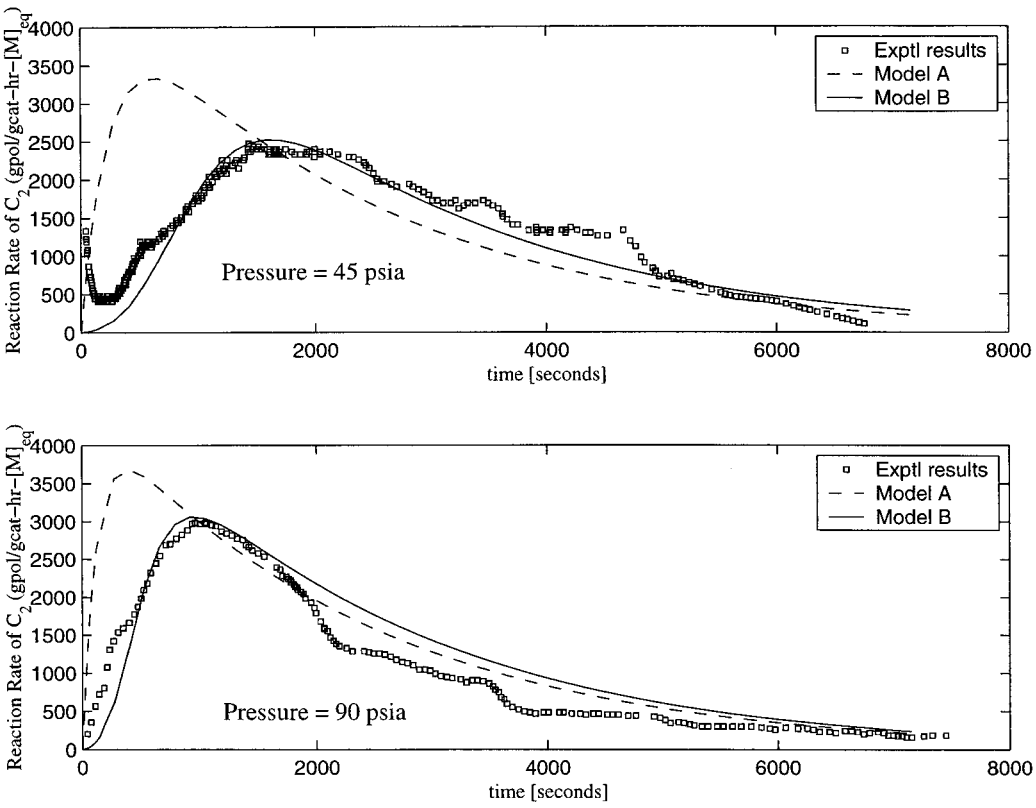

Figure 14 Model predictions versus experimental data at 80°C. Model A: Includes gas–liquid mass-transfer limitations. Model B: Accounts for gas–liquid mass-transfer and diffusion limitations.

$$V\frac{dC_{\text{act}}}{dt} = (\eta_l k_a C_{\text{pot}}[M_1]_{\text{eq}} - k_d C_{\text{act}})V - C_{\text{act}}\frac{dV}{dt} \tag{21}$$

$$V\frac{d\mu_0}{dt} = (\eta_l k_i C_{\text{vac}}[M_1]_{\text{eq}} - k_d C_{\mu 0})V - \mu_0\frac{dV}{dt} \tag{22}$$

$$V\frac{dC_{\text{dead}}}{dt} = (k_d C_{\text{act}})V - C_{\text{dead}}\frac{dV}{dt} \tag{23}$$

$$V\frac{d\lambda_1}{dt} = \eta_l(k_p\mu_0 + k_i C_{\text{vac}})[M_1]_{\text{eq}}V - \lambda_1\frac{dV}{dt} \tag{24}$$

The Appendix gives some additional details regarding the calculations of certain variables that appear in the set of ordinary differential equations. From this model, the ethylene consumption rate is determined by the following equation:

$$Rate = \eta_l(k_p\mu_0 + k_i C_{\text{vac}} + k_a C_{\text{pot}})[M_1]_{\text{eq}}\frac{V_{\text{swellamorph}}}{V} \tag{25}$$

The last factor in eq. (25) recognizes that only the monomer swollen into the amorphous phase of the polymer may react. The kinetic parameters in Table IV (obtained from gas-phase studies[1]) are used in model predictions. For the simulations, the value of C_{pot} was equal to 1.25×10^{-4}.

Model Predictions

Figures 10–14 contain the experimental data and predictions by model A (where only gas–liquid mass-transfer limitations are considered) and model B (where both gas–liquid mass-transfer and diffusion limitations are considered) for the different reaction conditions. At 62°C (see Fig. 10), model A predicts a slightly higher initial reaction rate compared to model B and the experimental data at the two operating

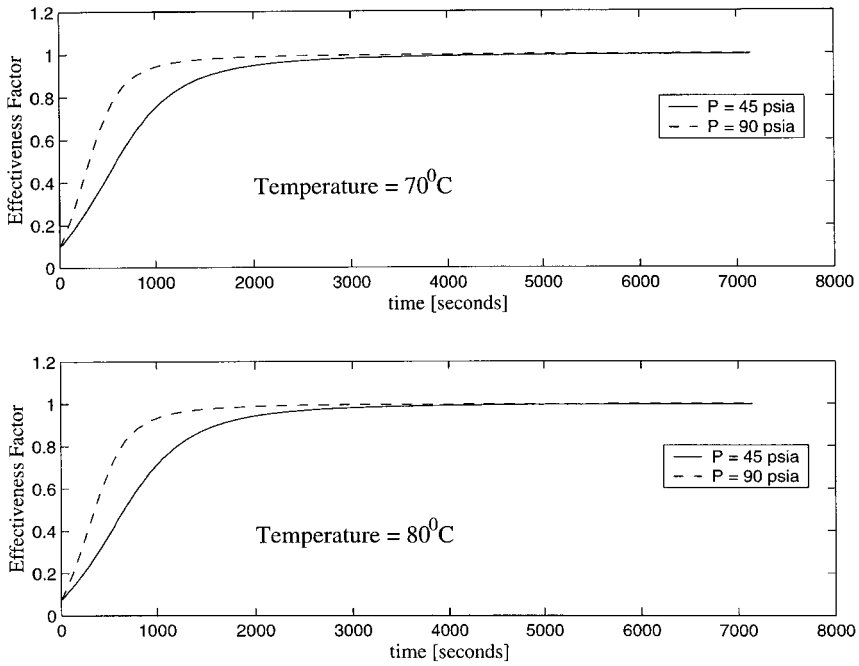

Figure 15 Intraparticle effectiveness factors as a function of time.

pressures. By contrast, at 70°C, Figures 11 and 12 show that failure to consider the presence of diffusion limitations result in model A, predicting a much higher initial reaction rate than what is observed with the experimental data. Comparatively, model B effectively captures the experimental trends at the different reaction pressures. Figures 13 and 14 provide the comparisons between the models and the experimental data for the different reaction pressures at a temperature of 80°C. The results further emphasize the need to account for diffusion as model A fails to capture the kinetic behavior during early reaction times. The model predictions prove that the presence of macroparticle diffusion limitations at early reaction times is the important difference between gas-phase and slurry polymerization. To further illustrate the significance of these diffusion limitations, Figure 15 provides plots of the intraparticle effectiveness factors as a function of time. The plots provide information on the duration of the reaction time, during which diffusion limitations are important. As the pressure increases, the time during which diffusion limitations are important decreases. This would be appropriate since a higher reaction pressure translates to a higher monomer concentration in the polymer and therefore the polymer particle grows at a faster rate. As the growth factor increases, the value of the Thiele modulus decreases and, subsequently, the effectiveness factor is closer to 1 at much shorter reaction times.

CONCLUSIONS

In this study, the kinetics of ethylene homopolymerization was investigated in a slurry reactor using a supported unbridged metallocene catalyst. The main objective was to be able to predict the slurry kinetic behavior using a model that contained catalyst kinetic parameters obtained from gas-phase studies. The slurry model included the effects of gas–liquid mass-transfer and diffusion limitations. It was found that failure to consider the presence of diffusion limitations would result in the loss of ability to predict slurry experimental trends at early reaction times using gas-phase parameters. The slurry model, accounting for macroparticle diffusion and containing the kinetic parameters from the gas phase, predicts the experimental trends rather well. This study is, to the best of our knowledge, the first time that slurry and gas-phase reactor behavior have been compared and modeled with the same kinetic parameters. This provides the groundwork for future studies dealing with copolymerization kinetics in both gas-phase and slurry reactors.

The authors would like to thank Andrew Ives for the assistance provided in troubleshooting various startup problems with the slurry reactor and Brian Banaszak for the assistance in determining the thermodynamic interaction parameters.

APPENDIX

Physical Parameters Used in the Model

Initial volume	1.5 L
d_{cat}	50 μ
Macroparticle diffusivity, D_l	3×10^{-6} cm^2/s
ρ_{cat} (g/cm^3)	2.33
ρ_{pol} (g/cm^3)	0.94
Swell (333 K)	0.43
Swell (343 K)	0.29
Swell (353 K)	0.21
CrysFrac	0.65

V_{liq} and $[M_i]_{liq}$ are calculated using a procedure that was previously implemented by Zacca[24]:

$$ConP = Mw(\lambda_1) \tag{A.1}$$

$$V_{pol} = V\frac{ConP}{\rho_{polym}} \tag{A.2}$$

$$V_{cryst} = CrysFrac(V_{pol}) \tag{A.3}$$

$$Swell = V_{sorbed\ species}/V_{pol} \tag{A.4}$$

$$V_{swellamorph} = \frac{(1 - CrysFrac)}{(1 - Swell)} V_{pol} \tag{A.5}$$

$$V_{liq} = V - V_{cryst} - V_{swellamorph} \tag{A.6}$$

$$[M_i]_{liq} = [M_i]_b \frac{V}{V_{liq}} \tag{A.7}$$

where $[M_i]_{liq}$ is the concentration of the monomer in the diluent, and $[M_i]_b$, the concentration of the monomer in the bulk (polymer + diluent). The swelling factors are estimates based on Henry's law. The value for *CrysFrac* was obtained from results obtained for HDPE.[5]

The density of the mixture, ρ_{mix}, is calculated by the following equation:

$$\frac{1}{\rho_{mix}} = \frac{w_{sol}}{\rho_{sol}} + \frac{w_{polym}}{\rho_{polym}} + \frac{w_{cat}}{\rho_{cat}} \tag{A.8}$$

NOMENCLATURE

C_{act}	concentration of the active sites (mol/cc-amor.polym.)
C_{cat}	concentration of the catalyst (mol/cc-soln)
C_{dead}	concentration of the dead sites (mol/cc-amor.polym.)
C_{pot}	concentration of potential sites (mol/cc-amor.polym.)
C_{vac}	concentration of vacant sites (mol/cc-amor.polym.)
D_l	macroparticle diffusivity (cm^2/s)
E_a	activation energy of site activation (kcal/mol)
E_p	activation energy of propagation (kcal/mol)
E_d	activation energy of deactivation (kcal/mol)
F_{in} and F_{out}	inflow and outflow of ethylene (cc/min)
k_La	mass-transfer coefficient (1/s)
k_a	kinetic constant for site activation (cc-amor.polym/mol.act-sites s^{-1})
k_p	kinetic constant for propagation (cc-amor.polym./mol.act-sites s^{-1})
k_d	kinetic constant for deactivation (1/s)
$[M_i]_{liq}$	concentration of the monomer in the diluent (mol/cc-soln)
$[M_i]_b$	concentration of the monomer in the bulk (mol/cc-bulk)
$[M_i]_{eq}$	equilibrium monomer concentration in the polymer (mol/cc-amor.polym.)
$[M_i]_{eql}$	equilibrium monomer concentration in diluent (mol/cc-soln)
p	partial pressure (atm)
R	universal gas constant (0.0802 L atm g^{-1} mol^{-1} K^{-1})
T	reactor temperature (K)
v_g	volume of the gas phase in the reactor (L)
v_i	volume fractions of a species in the polymer phase
V_{liq}	volume of the liquid phase in the reactor (cc)
V	total volume of reaction medium (solid + liquid) (cc)
V_i	partial molar volume of species i
V_{pol}	volume of polymer (cc)
V_{cryst}	volume of the crystalline fraction (cc)

$V_{\text{swellamorph}}$	volume of the swollen amorphous polymer (cc)
w_{sol}	weight fraction of the solvent
w_{polym}	weight fraction of the polymer
w_{cat}	weight fraction of the catalyst
δ_i	solubility parameter of component i $(\text{cal/cm}^3)^{1/2}$
γ	entropy correction factor
λ_1	first moment (bulk) (mol/cc)
μ_0	zeroth moment (live) (mol/cc)
μ_{is}	chemical potential of species i in the solvent phase
μ_{ip}	chemical potential of species i in the polymer phase
ψ	entropy parameter used to determine χ_{12}
θ	*theta* or *Flory temperature* used to determine χ_{12}
χ_{ij}	interaction parameter between species $i - j$
ρ_{sol}	density of the solvent (g/cc)
ρ_{pol}	density of the polymer (g/cc)
ρ_{cat}	density of the catalyst (g/cc)
ρ_{mix}	density of the mixture (g/cc)

REFERENCES

1. Xu, Z.; Chakravarti, S.; Ray, W. H. J Appl Polym Sci 2001, 80, 81–114.
2. Chakravarti, S.; Ray, W. H. J Appl Polym Sci 2001, 80, 1096–1119.
3. Han-Adebekun, G. C.; Debling, J. A.; Ray, W. H. J Appl Polym Sci 1997, 64, 373–382.
4. Debling, J. A. Ph.D. Thesis, University of Wisconsin, 1997.
5. Han-Adebekun, G. C.; Hamba, M.; Ray, W. H. J Polym Sci Part A Polym Chem 1997, 35, 2063–2074.
6. Hamba, M.; Han-Adebekun, G. C.; Ray, W. H. J Polym Sci Part A Polym Chem 1997, 35, 2075–2096.
7. Bray, W. S. Master's Thesis, University of Wisconsin, 1993.
8. Flory, P. J. Principles of Polymer Chemistry; Cornell University; Ithaca, NY, 1953.
9. Floyd, S.; Choi, K. Y.; Taylor, T. W.; Ray, W. H. J Appl Polym Sci 1986, 32, 2935–2960.
10. Chang, M.-Y.; Morsi, B. I. Chem Eng Sci 1991, 46, 2639–2650.
11. Floyd, S.; Hutchinson, R. A.; Ray, W. H. J Appl Polym Sci 1986, 32, 5451–5479.
12. Li, J.; Mizan, T. I.; Morsi, B. I.; Chang, M.-Y.; Maier, E. E.; Singh, C. P. P. Chem Eng Sci 1994, 49, 821–830.
13. Li, J.; Tekie, Z.; Mohammad, A.; Morsi, B. I. Can J Chem Eng 1996, 74, 87–91.
14. Li, J.; Mizan, T. I.; Morsi, B. I.; Maier, E. E.; Singh, C. P. P. Chem Eng Sci 1996, 51, 549–559.
15. Mallon, J. L. Master's Thesis, University of Wisconsin, 1996.
16. Pritchard, M.; Webb, G. B.; Rubin, L. C. Chem Eng Prog 1951, 47, 419.
17. Kissin, Y. V. Isospecific Polymerization of Olefins with Heterogeneous Ziegler–Natta Catalysts; Springer-Verlag: New York, 1987.
18. Hutchinson, R. A. Ph.D. Thesis, University of Wisconsin, 1990.
19. Chueh, P. L.; Prausnitz, J. M. AIChE J 1967, 13, 1099–1107.
20. Kay, W. B. Ind Eng Chem 1967, 40, 1459.
21. Gmehling, J.; Omken, U. Vapor Liquid Equilibrium Data Collection; Chemistry Data Series; DECHEMA: Frankfurt/Main, 1977–1990.
22. Young, R. J.; Lovell, P. A. Introduction to Polymers; Chapman and Hall: London, 1992.
23. Barton, A. F. M. Handbook of Polymer–Liquid Interaction Parameters and Solubility Parameters; CRC: Boca Raton, FL, 1990.
24. Zacca, J. J. Ph.D. Thesis, University of Wisconsin, 1995.